

Mössbauer spectroscopic and x-ray diffraction studies of structural and magnetic properties of heat-treated $(\text{Ni}_{0.5}\text{Zn}_{0.5})\text{Fe}_2\text{O}_4$ nanoparticles

De-Ping Yang^{a)} and Lindsey K. Lavoie

Physics Department, College of the Holy Cross, Worcester, Massachusetts 01610

Yide Zhang, Zongtao Zhang, and Shihui Ge

Inframat® Corporation, Willington, Connecticut 06279

(Presented on 13 November 2002)

Because of their high electrical resistivity and high magnetic permeability, nickel–zinc ferrites are among the best soft magnetic materials for high-frequency applications. In this work, a precursor of nanostructured $(\text{Ni}_{0.5}\text{Zn}_{0.5})\text{Fe}_2\text{O}_4$ was obtained by a sol–gel method modified for large quantity production. Six heat-treated samples were produced by calcining the precursor for 3 h at 450, 500, 600, 650, 700, and 1100 °C, respectively. X-ray diffraction peak width data have been used to estimate the particle sizes of the calcined samples. Room-temperature and low-temperature ^{57}Fe Mössbauer effect experiments allowed us to determine whether the heat-treated nanoparticles are crystalline or amorphous, whether there is a superparamagnetic phase, and which calcining temperature is optimum for obtaining a large magnetic hyperfine field and a homogeneous magnetic phase. Room-temperature Mössbauer spectra revealed that the precursor is paramagnetic, while the heat-treated samples have the ferrimagnetic phase. The samples heat treated at a calcining temperature of 650 °C or higher showed no residual paramagnetic phase, indicating that 650 °C is the threshold calcining temperature for homogeneous $(\text{Ni}_{0.5}\text{Zn}_{0.5})\text{Fe}_2\text{O}_4$ nanoparticles. A comparison between low-temperature and room-temperature Mössbauer spectra demonstrated that the precursor is paramagnetic, whereas the heat-treated (500 °C) sample has a component that shows superparamagnet relaxation. © 2003 American Institute of Physics.

[DOI: 10.1063/1.1540146]

I. INTRODUCTION

Nickel–zinc ferrite is a magnetic ceramic semiconductor with high electrical resistivity and high magnetic permeability, especially suitable for high-frequency applications. Its structural and magnetic properties have been extensively studied over the last five decades, and the material can be synthesized by numerous different chemical and physical methods. Recently, nanoparticle and thin-film ferrite materials have been produced by novel approaches such as chemical coprecipitation,¹ the sol–gel method,² hydrothermal processing,³ high-energy ball milling,⁴ pulsed-laser deposition,⁵ sputter deposition,⁶ and spin-spray plating.⁷ To study the magnetic properties of these new ferrite materials, ^{57}Fe Mössbauer spectroscopy provides a microscopic probe for the local magnetic and structural information.^{8,9} In this work, we have synthesized $(\text{Ni}_{0.5}\text{Zn}_{0.5})\text{Fe}_2\text{O}_4$ nanoparticles using the sol–gel method modified for large quantity production, and used x-ray diffraction and Mössbauer spectroscopy for characterization of the samples calcined at various temperatures. Room-temperature and low-temperature Mössbauer spectra provided information on the evolution of the magnetic phases in the material upon calcination and determined the optimum calcination temperature.

II. EXPERIMENTAL METHODS

Nanostructured $(\text{Ni}_{0.5}\text{Zn}_{0.5})\text{Fe}_2\text{O}_4$ was synthesized by a low-temperature approach based on the sol–gel autocombustion method.¹⁰ Appropriate amounts of nickel nitrate, zinc nitrate, and iron(III) citrate were dissolved in deionized water. Citric acid was added as a gelating agent. The clear solutions were mixed and slowly dried until the solution was concentrated. The mixture was further dried in an oven at 40 °C for 12 h, and porous agglomerates were obtained (precursor). A series of six Ni–Zn ferrite powder samples were obtained by calcining the precursor in controlled oxygen atmosphere for 3 h at 450, 500, 600, 650, 700, and 1100 °C, respectively.

^{57}Fe Mössbauer spectra were obtained using an Austin Science Associates constant-acceleration spectrometer with a 30 mCi source of ^{57}Co in a rhodium matrix. Sample temperatures below 295 K were obtained using a closed-cycle two-stage Displex helium refrigerator with a DMX-20 vibration–isolation interface (APD Cryogenics). The velocity scale was calibrated using a pure α -Fe foil absorber at room temperature. X-ray diffraction patterns were obtained by employing Cu $K\alpha$ radiation and a Philips x-ray diffractometer which was equipped with a single-crystal monochromator.

III. RESULTS AND DISCUSSION

X-ray diffraction patterns of the precursor and the six heat-treated samples are shown in Fig. 1. While the precursor

^{a)}Electronic mail: dyang@holycross.edu

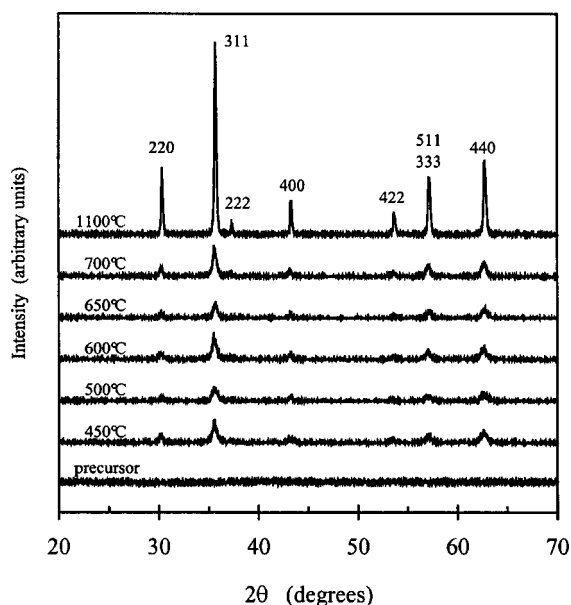


FIG. 1. X-ray diffraction patterns of the precursor and calcined samples of nanoparticle $(\text{Ni}_{0.5}\text{Zn}_{0.5})\text{Fe}_2\text{O}_4$, obtained using $\text{Cu K}\alpha$ radiation. The reflections are indexed to the cubic spinel ferrite structure with a lattice constant of 0.835 nm.

provides no diffraction peaks, the calcined samples clearly show the cubic spinel structure of Ni–Zn ferrite. The peaks become sharper and more pronounced for samples calcined at 650 °C or higher, indicating progressively better crystallization. Using the Scherrer equation,¹¹ the particle sizes have been estimated to be 19, 15, 18, 21, 22, and 40 nm for the samples calcined at 450, 500, 600, 650, 700, and 1100 °C, respectively. The lattice constant has been found to be 0.835 nm, typical of Ni–Zn ferrite.^{9,12,13}

Ni–Zn ferrite crystallizes in the spinel structure based on a face-centered-cubic lattice of oxygen ions, with the metallic ions occupying 8 tetrahedral sites and 16 octahedral sites. Each unit cell contains eight formula units of $(\text{Ni}_{0.5}\text{Zn}_{0.5})\text{Fe}_2\text{O}_4$. It is well known that Zn^{2+} prefers the tetrahedral (A) sites and Ni^{2+} prefers the octahedral (B) sites,⁹ and a recent combined study using extended x-ray absorption fine structure and Mössbauer effect confirmed that it is also the case in nanosized Ni–Zn ferrite.¹² Therefore, 1/2 of the A sites are occupied by Zn^{2+} and 1/4 of the B sites by Ni^{2+} . The Fe^{3+} ions occupy both A and B sites in the ratio of 1:3. While Fe^{3+} and Ni^{2+} are magnetic ions, Zn^{2+} is nonmagnetic. The A and B magnetic ions are engaged in a superexchange, giving rise to the ferrimagnetic nature of the material.

For an ^{57}Fe ion at the tetrahedral A site, its metallic ion neighbors at B sites are all magnetic (on an average, 3Fe–1Ni). Therefore, the hyperfine field at the A-site ^{57}Fe nuclei should be relatively constant. For a B-site ^{57}Fe , however, its six metallic ion neighbors at A sites may include any number of nonmagnetic Zn^{2+} ions (e.g., 6Fe–0Zn, 5Fe–1Zn, 4Fe–2Zn, . . . , 0Fe–6Zn), and the hyperfine field is reduced due to the presence of Zn^{2+} ions. Assuming a random distribution of Zn^{2+} ions, the probability of having n Zn^{2+} ions ($0 \leq n \leq 6$) is given by the binomial formula

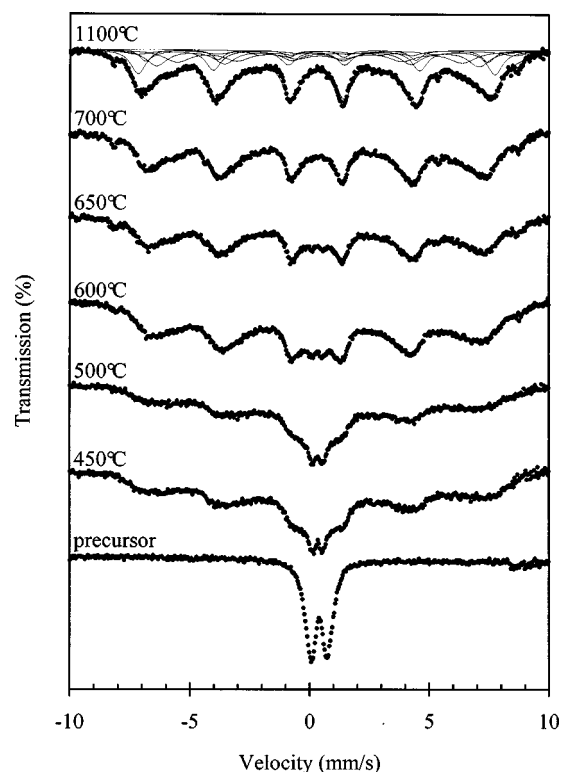


FIG. 2. Room-temperature ^{57}Fe Mössbauer spectra of nanoparticle $(\text{Ni}_{0.5}\text{Zn}_{0.5})\text{Fe}_2\text{O}_4$ samples. The calcining temperatures are indicated next to the spectra of the heat-treated samples. Also shown for the well-crystallized sample are six subspectra corresponding to Fe^{3+} at the A site as well as at B sites with 1, 2, 3, 4, and 5 Zn^{2+} neighbors, respectively.

$$P(n, x) = \frac{6!}{n!(6-n)!} x^n (1-x)^{6-n},$$

where x is the average fraction of A sites occupied by Zn^{2+} . In our case, $x=0.5$, and the probabilities are 0.016, 0.094, 0.234, 0.313, 0.234, 0.094, and 0.016 for $n=0, 1, 2, 3, 4, 5,$ and 6, respectively. Mössbauer effect studies of conventional and nanostructured Ni–Zn ferrites have provided evidence for the B-site hyperfine distribution according to these probabilities.^{12,14–17}

In this work, the Mössbauer spectra from the calcined samples have been fit using one A-site sextet and five B-site sextets (the probabilities for $n=0$ and $n=6$ are not large enough to be significant). Figure 2 shows the room-temperature Mössbauer spectra from the precursor and the calcined samples. For the sample calcined at 1100 °C, the hyperfine field at the A site is 46.3 T, and those at the B sites are 48.9, 44.4, 41.9, 37.0, and 19.8 T corresponding to having 1, 2, 3, 4, and 5 nonmagnetic Zn^{2+} neighbors. The typical linewidth is about 0.5 mm/s, reflecting certain degree of disorder, due to surface effects and structural straining. The spectrum from the precursor shows a quadrupole doublet, indicating its nonmagnetic nature. As the calcining temperature goes higher, the magnetic component increases, and the paramagnetic one diminishes. When calcined at 650 °C or higher, the spectrum is composed of pure magnetic sextets, indicating that 650 °C is the threshold calcining temperature for homogeneous $(\text{Ni}_{0.5}\text{Zn}_{0.5})\text{Fe}_2\text{O}_4$ nanoparticles.

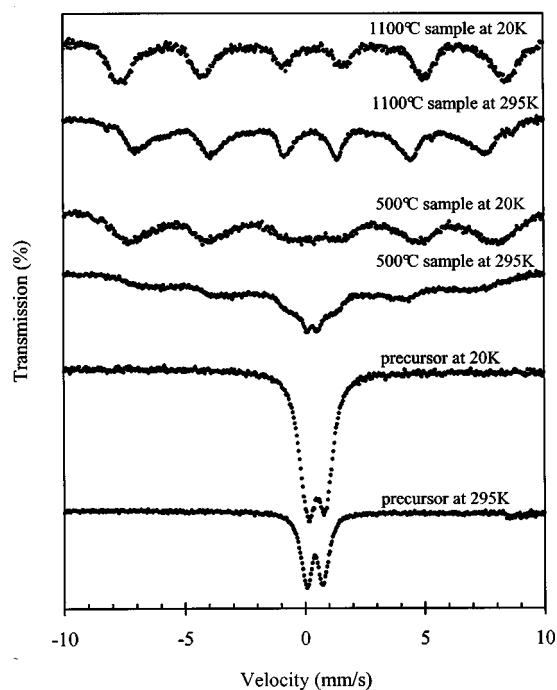


FIG. 3. Comparison of low-temperature and room-temperature Mössbauer spectra of three of the nanoparticle $(\text{Ni}_{0.5}\text{Zn}_{0.5})\text{Fe}_2\text{O}_4$ samples. The precursor is paramagnetic, the sample calcined at 500°C exhibits superparamagnetic relaxation, and the well-crystallized sample shows ferrimagnetic behavior at all temperatures investigated.

Low-temperature Mössbauer spectra from three samples are shown in Fig. 3. By comparison with their room-temperature spectra, we see that each has a different magnetic behavior. The precursor is completely paramagnetic as evidenced by the same doublet in its room-temperature and low-temperature spectra. The sample calcined at 500°C shows superparamagnetic relaxation as evidenced by the emergence of magnetic sextets at low temperatures, at the expense of the doublet as observed in the room-temperature spectrum. The well-crystallized sample (1100°C), however, does not have superparamagnetic behavior, due to its larger particle size, and both its room-temperature and low-temperature spectra show similar magnetic sextet distributions, except for larger hyperfine field values at 20 K, as expected.

In summary, x-ray diffraction and Mössbauer spectroscopy have been applied to characterize nanosized

$(\text{Ni}_{0.5}\text{Zn}_{0.5})\text{Fe}_2\text{O}_4$ synthesized by the sol-gel method modified for large quantity production. The minimum calcining temperature for obtaining a homogeneous ferrimagnetic phase is 650°C and the corresponding particle size is 21 nm. The ^{57}Fe Mössbauer spectra for samples calcined at 650°C or higher can be fit by one sextet for the A site and a binomial distribution of sextets for the B sites with different numbers of Zn^{2+} ion neighbors. This indicates that nanoparticles of $(\text{Ni}_{0.5}\text{Zn}_{0.5})\text{Fe}_2\text{O}_4$ have a similar crystalline and magnetic structure as the conventional Ni-Zn ferrite, except for surface effect and straining, characteristics of nanosized particles. The Ni-Zn ferrite materials produced by this method can be scaled to large production. The nanoparticle Ni-Zn ferrite may also be made as embedded in an insulating matrix such as amorphous SiO_2 , which would further reduce eddy current losses for high-frequency applications.

ACKNOWLEDGMENT

The authors gratefully acknowledge a Cottrell College Science Award from Research Corporation (CC4022) for providing the low-temperature Mössbauer apparatus.

- ¹H. Tang, Y. W. Du, Z. Q. Qiu, and J. C. Walker, *J. Appl. Phys.* **63**, 4105 (1988).
- ²L. L. Hench and J. K. West, *Chem. Rev.* **90**, 33 (1990).
- ³A. Dias, N. D. S. Mohallem, and R. L. Moreira, *J. Phys.* **III 6**, 843 (1996).
- ⁴J. S. Jiang, L. Gao, X. L. Yang, J. K. Guo, and H. L. Shen, *J. Mater. Sci. Lett.* **18**, 1781 (1999).
- ⁵F. W. Oliver, D. Seifu, E. Hoffman, D. B. Chrisey, J. S. Horwitz, and P. C. Dorsey, *Appl. Phys. Lett.* **75**, 2993 (1999).
- ⁶M. Desai, S. Prasad, N. Venkataramani, I. Samajdar, A. K. Nigam, N. Keller, R. Krishnan, E. M. Baggio-Saitovitch, B. R. Pujada, and A. Rossi, *J. Appl. Phys.* **91**, 7592 (2002).
- ⁷N. Matsushita, C. P. Chong, T. Mizutani, and M. Abe, *J. Appl. Phys.* **91**, 7376 (2002).
- ⁸J. M. Daniels and A. Rosencwaig, *Can. J. Phys.* **48**, 381 (1970).
- ⁹L. K. Leung, B. J. Evans, and A. H. Morrish, *Phys. Rev. B* **8**, 29 (1973).
- ¹⁰A. Verma, T. C. Goel, and R. G. Mendiratta, *Mater. Sci. Technol.* **16**, 712 (2000).
- ¹¹B. E. Warren, *X-ray Diffraction* (Dover, New York, 1990), p. 253.
- ¹²A. S. Albuquerque, J. D. Ardisson, W. A. A. Macedo, and M. C. M. Alves, *J. Appl. Phys.* **87**, 4352 (2000).
- ¹³L. Wang and F. S. Li, *J. Magn. Magn. Mater.* **223**, 233 (2001).
- ¹⁴T. A. Dooling and D. C. Cook, *J. Appl. Phys.* **69**, 5352 (1991).
- ¹⁵M. Arshed, M. Siddique, M. Anwar-ul-Islam, N. M. Butt, T. Abbas, and M. Ahmed, *Solid State Commun.* **93**, 599 (1995).
- ¹⁶W. C. Kim, S. J. Kim, Y. R. Uhm, and C. S. Kim, *IEEE Trans. Magn.* **37**, 2362 (2001).
- ¹⁷M. A. Amer and M. El Hiti, *J. Magn. Magn. Mater.* **234**, 118 (2001).